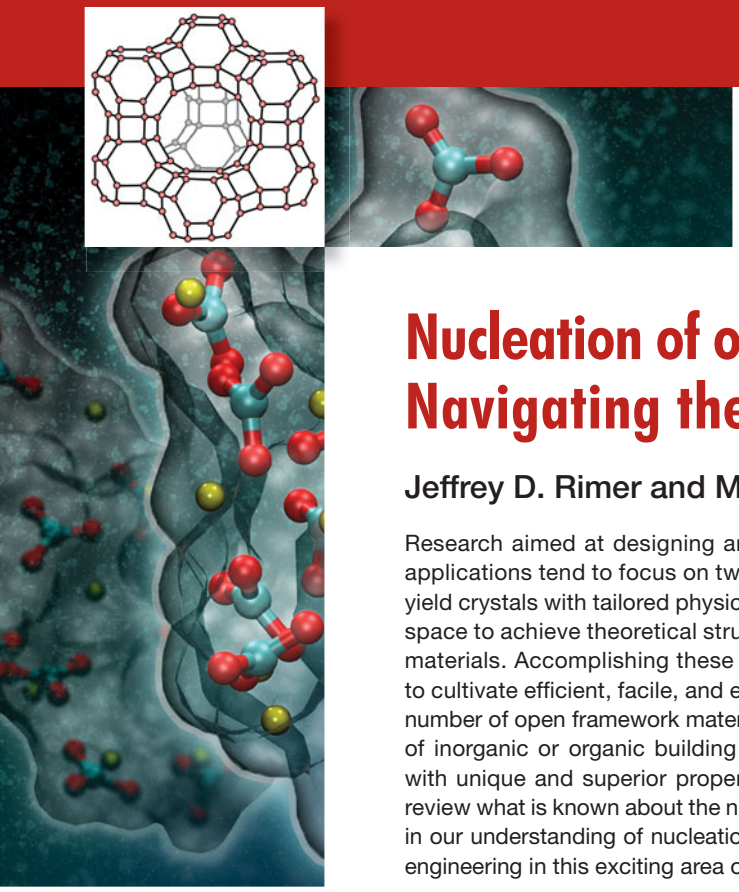


Nucleation of open framework materials: Navigating the voids

Jeffrey D. Rimer and Michael Tsapatsis

Research aimed at designing and optimizing open framework materials for commercial applications tend to focus on two critical objectives: identifying synthesis conditions that yield crystals with tailored physicochemical properties, and unlocking the untapped design space to achieve theoretical structures that far outnumber the list of synthetically realized materials. Accomplishing these goals requires detailed knowledge of nucleation in order to cultivate efficient, facile, and economical methods of controlling crystallization. The vast number of open framework materials that can be engineered through the judicious selection of inorganic or organic building units hold the promise for future discovery of materials with unique and superior properties compared to available porous materials. Herein, we review what is known about the nucleation of open framework crystals, highlighting the voids in our understanding of nucleation pathways, and we offer guidelines for advancing crystal engineering in this exciting area of research.

Introduction

Porous crystalline materials form in nature as minerals. Synthetically, they can be produced as a variety of organic, inorganic, and hybrid structures with applications in gas storage, catalysis, separations, adsorption, drug delivery, etc. There are three general classes of open framework materials: zeolites and related zeotypes, metal–organic frameworks (MOFs), and covalent–organic frameworks (COFs).

Zeolites are microporous aluminosilicates composed of covalently bound tetrahedral networks (i.e., T–O–T bonds where the tetrahedral site T = Si or Al), as shown in **Figure 1**a. Zeolite framework types are referred to by a three-letter code that was assigned for each unique topology by the International Zeolite Association Structure Commission.[1] Zeotypes, such as aluminophosphates (AlPOs) and silicoaluminophosphates (SAPOs), are isostructural analogues of zeolites with a broad range of heteroatoms (e.g., T = Ge, Ga, Sn, B, P, etc.). Other variations exist, including titanosilicate molecular sieves. MOFs are coordination compounds formed from metals and organic linkers (Figure 1b).[2] A practically unmatched design space for constructing unique MOFs by interchanging linkers has led to the discovery of many libraries of materials.[3] COFs are derived from the covalent interconnection of building blocks, as shown in Figure 1c.[4]

Additional porous materials include clathrates (or inclusion compounds), which are polymeric materials stabilized by the presence of guest molecules that occupy the void space in the crystal structure (rendering these materials essentially nonporous). Host–guest crystals with supramolecular cages occupied by an array of occluded molecules can also be prepared from building units that form hydrogen-bonded networks.[5] In this article, we restrict our discussion to the nucleation of open frameworks (i.e., free of occluded guest molecules), focusing predominantly on zeolites, with some discussion of MOFs and COFs.

Open framework materials provide a diverse platform in crystal engineering where physicochemical properties, such as pore size, volume, geometry, and molecular functionality, can be tailored for target applications.[6–11] Theoretically, there are hundreds of thousands of zeolite structures (**Figure 2**a)[12,13] and even more MOFs[14] that are thermodynamically stable and, in principle, can be synthetically realized provided suitable synthesis conditions are identified. This task, however, is nontrivial. For example, around 230 zeolite frameworks have been synthetically realized among the thousands of hypothetical structures. The majority of zeolite syntheses require the assistance of an organic structure-directing agent (OSDA). As illustrated in Figure 2b,[15] OSDAs are molecules with size and shape commensurate with the channels and cages of the crystal structure and thus facilitate zeolite crystallization. In the absence of OSDAs, only about 50 natural and 30 synthetic zeolite structures are known to exist or have been

Jeffrey D. Rimer, Department of Chemical and Biomolecular Engineering, University of Houston, USA; jrimer@central.uh.edu
Michael Tsapatsis, Department of Chemical Engineering and Materials Science, University of Minnesota, USA; tsapa001@umn.edu
doi:10.1557/mrs.2016.89

© 2016 Materials Research Society

https://doi.org/10.1557/mrs.2016.89 Published online by Cambridge University Press

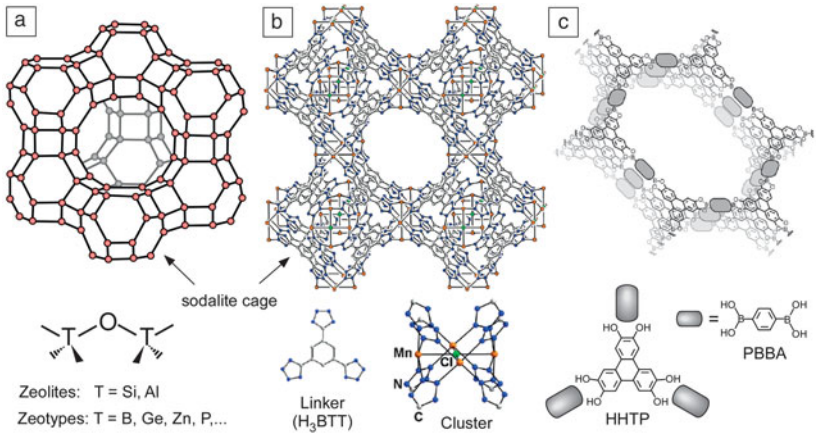


Figure 1. Examples of open framework crystals. (a) Zeolites and zeotypes are composed of tetrahedral (T) sites occupied by Si, Al, and other heteroatoms (shown here is faujasite [FAU framework type]). (b) Metal–organic frameworks (MOFs) are composed of metals coordinated with organic linkers. Illustrated here is the MOF-5 structure with a secondary building unit (sodalite cage) is similar to that in zeolite FAU. MOF-5 contains the tritopic ligand 1,3,5-tris(2*H*-tetrazol-5-yl)benzene (H_3BTT) and a Mn_4Cl cluster surrounded by eight tetrazolate rings. Adapted with permission from Reference 2. © 2006 American Chemical Society. (c) Covalent–organic frameworks (COFs) are composed of building blocks, illustrated here for COF-5, which is a boronate ester framework with the 2,3,6,7,10,11-hexahydroxytriphenylene (HHTP) building block and 1,4-phenylenebis(boronic acid) (PBBA) linker. Adapted with permission from Reference 4. © 2015 Royal Society of Chemistry.

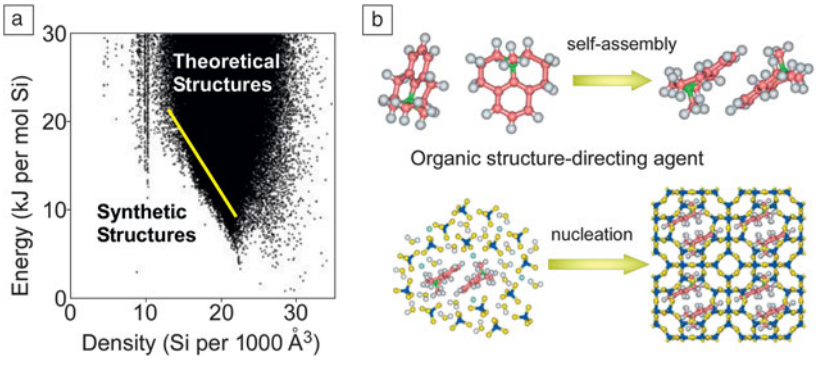


Figure 2. Diversity of zeolite frameworks. (a) The thermodynamic energy of ca. 300,000 hypothetical siliceous zeolite structures is plotted as a function of framework density. The yellow line subdivides the plot into synthetically realized (bottom left) and theoretical (upper right) structures. The relatively few structures in the former category highlight the synthetic challenge associated with realizing new zeolite structures. Adapted with permission from Reference 12. © 2015 Nature. (b) Example of the organic structure-directing agent 4-methyl-2,3,6,7-tetrahydro-1H,5H-pyrido [3.2.1-ij] quinolinium used to direct the formation of zeolite ITQ-29 (LTA framework type). Color code: C (red), H (white), O (yellow), N (green), and Si (blue). Adapted with permission from Reference 15. © 2004 Nature.

successfully produced in the lab.[16] The capability to access more theoretical zeolite structures depends on the ability to design OSDAs *a priori* with specificity for controlling the kinetic pathway of nucleation.

Similarly, new MOF structures rely on the appropriate selection of metal-linker building blocks. A computational study by Snurr, Hupp, and co-workers[17] showed that ca. 140,000 hypothetical MOF structures can be derived from a library of only 102 modular molecular building blocks. In many cases, the structural integrity of these materials relies on the presence of a solvent; upon its removal, the porous structure is often compromised. To this end, there are many open-ended questions regarding the nature of structure direction in porous materials, be it the influence of an OSDA, solvent molecule, inorganic ion, or other species present in growth solutions of open framework materials.

Computational screening of hypothetical open framework structures establishes boundaries for crystal engineering; however, there is a substantial void in our understanding of fundamental processes governing nucleation and growth that hinders the development of synthetic protocols to access this untapped design space. In this article, we summarize what is currently known in this field and highlight knowledge gaps in the mechanism(s) of nucleation that must be addressed in order to rationally design new and improved materials for existing and emerging applications.

Mechanisms of nucleation

Very little is known about the mechanisms of COF and MOF nucleation. One study on COF-5[18] suggests that monomers or small oligomers are involved in growth (**Figure 3**a), which could imply that the nucleation of COF-5 (and possibly other COFs) occurs by processes that are more closely aligned with classical nucleation theory (CNT) (see the Introductory article in this issue). MOFs are prepared using molecularly dispersed metals and ligands and thus have the potential to nucleate by a similar mechanism. Few reports in the literature address COF and MOF nucleation; to our knowledge, there are no studies identifying the presence of precursors (e.g., clusters or primary particles) in synthesis solutions that would allude to nonclassical pathways of COF or MOF crystallization.[19]

On the other hand, there is more information on zeolite nucleation; however, molecular-level details are generally lacking, and few structures have been studied, leaving many fundamental questions unanswered. One defining feature of zeolite synthesis is the formation of precursors, which include primary particles (1–6 nm), bulk aggregates (0.1–1 μm), and gels. Zeolite nucleation does not appear to involve the association of monomers/oligomers into clusters of critical size, as per CNT.[20] The ubiquitous presence of precursors in zeolite growth solutions[21] suggests a two-step mechanism of nucleation,[22,23] wherein the assembly of precursors provides a

https://doi.org/10.1557/mrs.2016.89 Published online by Cambridge University Press

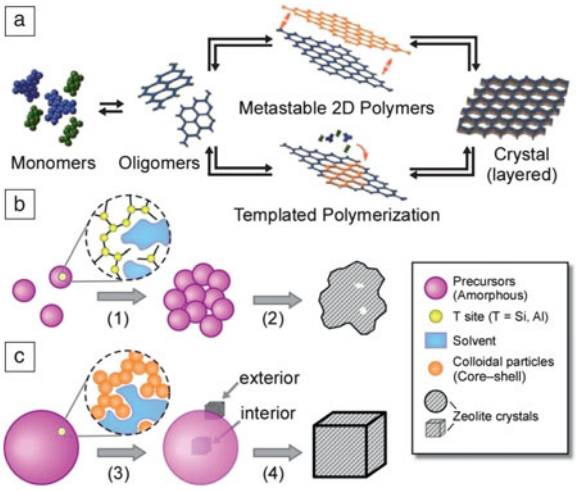


Figure 3. Putative pathways of nucleation for open framework crystals. (a) Dichtel and co-workers propose that COF-5 (covalent–organic framework) nucleation occurs through the assembly of monomers and oligomers, which also serve as growth units for 2D crystal growth. Adapted with permission from Reference 18. © 2006 American Chemical Society. (b) One pathway of zeolite nucleation involves the aggregation of primary particles (step 1) followed by their structural rearrangement (step 2) into the crystalline product. During this process, the nuclei maintain a size and shape that is similar to the amorphous aggregate. The crystals may contain voids or defects (e.g., misaligned domains). The primary particles are composed of (alumino)silicate polymers with entrained solvent (callout illustration). (c) A second pathway of zeolite nucleation involves the formation of bulk (sol-gel) amorphous aggregates (step 3). These particles serve as sites for heterogeneous nucleation, either on the exterior surface of gels or within their interior. Gels contain entrained solvent (callout illustration), and the (alumino)silicate within the gel serves as a nutrient for zeolite growth. During crystallization, the amorphous gel is consumed (step 4), often leading to crystal sizes that are commensurate with those of the original gel particles.

substrate for heterogeneous nucleation or potentially generates localized regions of high-solute (silica and alumina) concentration, which lowers the energetic barrier for nucleation.

The amorphous-to-crystalline transition in zeolite precursors is not well understood. This process can be subdivided into two nucleation pathways (Figure 3b–c) that are distinguished on the basis of the initial (alumino)silicate connectivity. Primary particles are composed of branched polymeric networks with many uncoordinated bonds (e.g., SiOH groups) and a significant fraction of solvent.[24–26] As shown in Figure 3b, nucleation often involves the aggregation of primary particles, followed by structural rearrangement into a nucleus through unknown molecular events and dynamic sequences. The majority of zeolite growth solutions are composed of amorphous gel particles (50 nm–1 μm), see Figure 3c. Gel particles often contain heterogeneous compositions with spatially segregated Si- and Al-rich domains,[27,28] suggesting that nucleation within gels involves significant bond breakage to form zeolite crystals. There are two general locations where nucleation occurs in gel particles: within the gel interior and on its exterior surface.[29,30]

The complexity of nucleation in gels renders these systems more difficult to characterize, therefore, our discussion will focus on studies of sols (i.e., pathway in Figure 3b) that constitute the basis of our understanding of zeolite nucleation.

Experimental and computational studies of zeolite nucleation

One of the most widely studied zeolites is silicalite-1 (siliceous MFI framework type), which is prepared from clear growth solutions that enable facile *in situ* characterization by scattering and microscopy techniques. Amorphous precursors of silicalite-1 are the primary particles (**Figure 4**a–b) that range in size from 1–6 nm, depending on the pH of the growth solution,[31–33] and have a core–shell arrangement with a silica-rich core and an OSDA-rich shell[24,32,34] with no evidence of the silicalite-1 structure. Recently, Auerbach and Monson used a reaction ensemble Monte Carlo method to model the self-assembly of silica in the presence of OSDA (Figure 4c), which provided insights on the ring-size distribution and OSDA location.[35] Their results are in agreement with the conclusions drawn from small-angle x-ray scattering and small-angle neutron scattering experiments by Rimer, Lobo, and Vlachos in that they indicate the absence of the silicalite-1

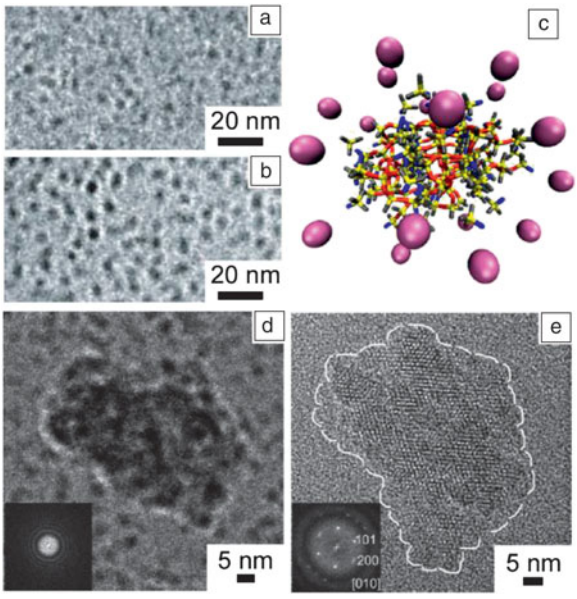


Figure 4. Nucleation of zeolite silicalite-1 (MFI framework type). Cryogenic transmission electron microscope (cryo-TEM) images[31] of (a) fresh primary particles and (b) after 180 days of aging at room temperature reveal structural evolution. (c) Snapshots of particles with an ordered arrangement of silica and organic structure-directing agent (OSDA) from reaction ensemble Monte Carlo simulations. Color code: Si (yellow), oxide (blue), bridging oxygen (red), hydroxyl (gray), and OSDA (purple). Reproduced with permission from Reference 35. © 2015 American Chemical Society. (d–e) Cryo-TEM images[38] of samples extracted at periodic times reveal the amorphous-to-crystal transformation of ca. 20-nm aggregates of precursors: (d) 200 days and (e) 220 days at room temperature. Insets are selected-area electron diffraction patterns.

https://doi.org/10.1557/mrs.2016.89 Published online by Cambridge University Press

crystal structure within the nanoparticles.[36,37] It appears that the silica nanoparticles are a metastable form of the silica-OSDA assembly with slow dynamics of evolution toward the silicalite-1 structure.

Cryogenic transmission electron microscopy (cryo-TEM) was used to track the evolution of precursors during crystallization at room temperature, and revealed a sequence of events (depicted in steps 1 and 2 of Figure 3b) that started with the aggregation of precursors (Figure 4d).[38] The experiments were performed at room temperature, where the disparity of time scales of silica assembly (seconds or less) with the very slow emergence of aggregates (months) were highlighted. Selected-area electron diffraction and high-resolution TEM imaging revealed these aggregates to be amorphous; however, increased synthesis time resulted in an amorphous-to-crystalline transition that was marked by the appearance of lattice fringes in cryo-TEM images (Figure 4e).[31] After a relatively short time (compared to the time it took for aggregation to be detected), the aggregates became fully crystalline with a size and shape comparable to those of the original aggregate. Void spaces were detected in the nuclei, which correspond to interstitial spaces within the aggregates.

It was also observed that nuclei are predominantly single crystals, where domains (i.e., regions corresponding to original precursors in the aggregate) share the same crystallographic orientation. Misaligned domains are occasionally observed. Such domains are detected in bulk crystals of zeolite ZSM-5 (MFI framework type) as intergrowths,[39] and they have also been documented for other nanocrystalline materials that grow through attachment of crystalline[40] or amorphous particles. In some cases, lattice strain at these defect sites may induce temporal reorientation, similar to Ostwald ripening of misaligned particles observed during iron oxyhydroxide crystallization by oriented attachment.[41]

The two-step mechanism of nucleation involves (1) the assembly of precursors and (2) their transformation into nuclei. As previously described, the first step appears to be well understood, but the second step is invariably complex and likely consists of numerous kinetic barriers, many of which may be energetically indistinguishable. Specifically, these processes involve bond breakage and formation, exchange of (alumino)silicate species between the precursor and growth solution, and the assembly of silicate monomers and fragments, including composite building units (CBUs) that correspond to repeating structures (e.g., cages or chains) of the crystalline framework.

Many computational studies in the literature examine the polymerization of (alumino)silicate clusters and the formation of rings and CBUs.[35,42–46] A common hypothesis in the literature is that zeolite crystals grow by the direct attachment of CBUs;[47] however, there is no direct evidence to support this mechanism. Much of the experimental data used to support these theories are derived from spectroscopic measurements (i.e., Fourier transform infrared, nuclear magnetic resonance, Raman, mass spectrometry) showing progressive changes in the connectivity of (alumino)silicate species during the induction period.[48–50] The temporal appearance or disappearance of rings, CBUs, and other oligomeric species provides evidence that structural changes occur. Linking these observations to the molecular processes of nucleation is a more difficult task. From the experimental standpoint, we should seek conditions where nucleation is not rare and fast (i.e., model systems where nucleation happens simultaneously throughout the crystallizing sols), such that changes in solution and nanoparticle structures (determined by the aforementioned techniques) can be correlated with the onset of nucleation. From the modeling standpoint, bridging approximate methods capable of describing silica polymerization and network formation[51] with more accurate descriptions of silica speciation in the presence of OSDA[52] could provide quantitative predictions of nucleation kinetics.

Polymorphism and intercrystalline conversions

Navrotsky and co-workers performed calorimetry studies and demonstrated that the enthalpies of formation ΔH_f for microporous zeolites[53] and MOFs[54] with pore diameters less than 2 nm exhibit an approximately linear relationship with framework molar volume $\underline{V}$; however, there is very little difference in ΔH_f among the different framework types (i.e., values differ by less than 10 kJ/mol). This similarity in enthalpy can result in the formation of polymorphs, which is commonly observed in MOF and zeolite synthesis. For example, there are multiple structures that can form during the preparation of zeolitic imidazolate frameworks (ZIFs) from solutions of zinc and imidazole (IM). As shown in **Figure 5**a, four different crystal structures—ZIF-2, ZIF-3, ZIF-6, and ZIF-10—can be prepared with identical composition, $Zn(IM)_2$, as a result of subtle changes in the synthesis conditions, such as temperature and solvent.[55] This alludes to the important role of kinetics in nucleation.

Notably, there are multiple kinetic barriers that must be overcome during the amorphous-to-crystalline transition in the two-step nucleation mechanism leading to the formation of secondary building units. A multitude of parameters can be manipulated in zeolite and MOF synthesis to alter the nucleation pathway. Establishing deterministic models or heuristic guidelines to control nucleation pathways *a priori* is one of the more challenging objectives in this field of research.

A common phenomenon during the crystallization of open framework materials illustrates the Ostwald–Lussac rule of stages (or Ostwald step rule),[56] which states that the first crystal to form is a metastable structure that undergoes a series of intercrystalline transformations leading to structures that are more thermodynamically stable. In the context of Navrotsky's calorimetry experiments, the trajectory of these transformations is toward denser framework structures (i.e., lower $\underline{V}$). For example, the synthesis of MOF-5 under cathodic bias (Figure 5b) occurs in three stages involving the initial formation of two layered structures prior to the formation of the final MOF-5 crystal.[57] Intercrystalline transformations in zeolite synthesis are more commonly observed in OSDA-free growth

https://doi.org/10.1557/mrs.2016.89 Published online by Cambridge University Press

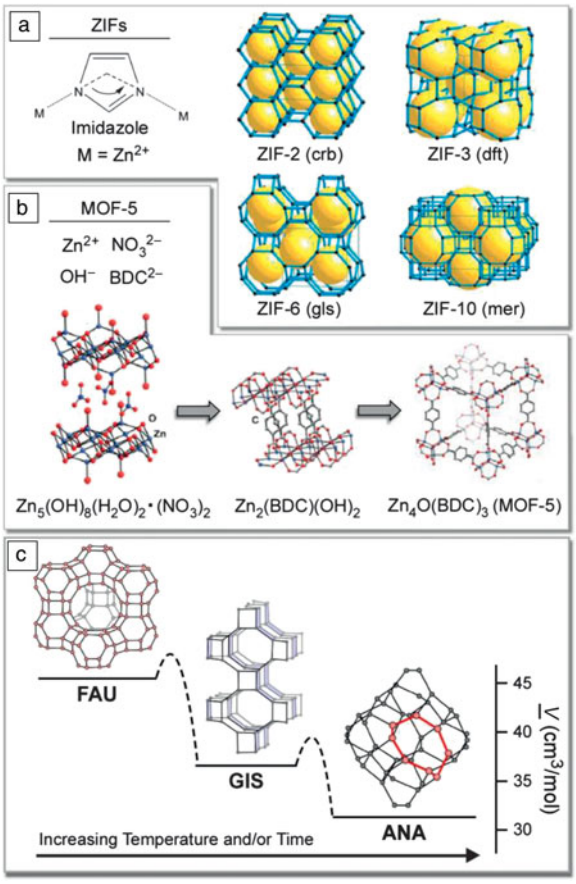


Figure 5. Examples of polymorphism for open framework materials. (a) Polymorphs of zeolitic imidazolate frameworks (ZIFs) with $Zn(IM)_2$ composition (IM is imidazole). Black dots indicate Zn, blue lines are IM, and yellow spheres highlight open voids (cages) within the pores. The kinetic pathways leading to the nucleation and growth of these four structures is altered by subtle changes in synthesis parameters. The three-letter abbreviations in parentheses refer to the framework structure. Adapted with permission from Reference 55. © 2006 National Academy of Sciences. (b) Example of intercrystalline conversions leading to the formation of MOF-5 (metal–organic framework), which is composed of 1,4-benzenedicarboxylate (BDC) linkers. Dincă and co-workers showed that electrochemically induced growth led to the formation of two intermediates prior to the transformation to MOF-5 product. Adapted with permission from Reference 57. © 2015 American Chemical Society. (c) The thermodynamic driving force for intercrystalline transformations in zeolite synthesis is governed by the progressive transition from initially metastable structures to those that are more thermodynamically stable (i.e., dense) structures. Rimer and co-workers reported the FAU-to-GIS-to-ANA transition that occurs with increased synthesis temperature or time.[27] Note: FAU, faujasite; GIS, gismondine; ANA, analcime; $\underline{V}$, molar volume.

solutions where alkali metals are used as inorganic structure-directing agents. An example of the Ostwald step rule for Na^+ zeolites is shown in Figure 5c involving the transition from faujasite (FAU framework type), a common metastable zeolite, to gismondine (GIS), and then analcime (ANA) with increasing synthesis temperature.[27] During these transformations, the initial formation of one zeolite is followed by nucleation of a second zeolite, which progressively grows in favor of a decreasing population of the initial (more metastable) structure.

These examples suggest that nucleation of certain zeolites is favored by the formation/presence of more metastable zeolites. The driving force for intercrystalline transformation is not well understood. Some transformations occur between zeolite structures with similar building units;[58] however, the three zeolite structures in Figure 5c do not share a common CBU. One possible explanation is an epitaxial relationship among zeolite structures wherein the crystal interface of the newly formed zeolite preferentially nucleates on a crystallographic face of the preexisting zeolite surface. Alternatively, the temporal change in growth solution composition during the crystallization of the metastable zeolite creates an environment that could potentially promote nucleation of the new phase. In many respects, intercrystalline transformation is analogous to seeded growth—a topic that is garnering increased attention in zeolite synthesis.[59,60] Developing a fundamental understanding of these processes could lead to improved methods of controlling nucleation pathways.[61]

Conclusions and outlook

We have presented an overview of the potential nucleation pathways of open framework crystals, focusing specifically on three classes of materials: zeolites, MOFs, and COFs. The topic of nucleation has received little attention in the MOF and COF literature; this presents an opportunity for future advancements in these areas of research. It is reasonable to believe that crystallization from growth solutions composed of small organic molecules and metal ions involves classical monomer-by-monomer addition; however, there exists a possibility that precursors (e.g., clusters or oligomers) form during the induction period and facilitate nucleation. The number of crystalline materials that are either known or postulated to grow by nonclassical routes involving crystallization by particle attachment (CPA)[19] is continually expanding. It is entirely feasible that MOF and COF crystals could be added to this list of materials.

Knowledge of zeolite growth by CPA dates back to the 1990s, when primary particles were first identified in silicalite-1 syntheses.[62,63] Difficulties imposed by zeolite synthesis conditions, however, render *in situ* characterization of nucleation and crystal growth challenging. To this end, observing zeolite nucleation at the length and time scales necessary to reconcile mechanistic uncertainties with molecular-level resolution remains elusive, but characterization and modeling methodologies have reached a level of maturity that, if applied to an appropriate system, could soon provide the first molecular-level quantitative description of zeolite nucleation kinetics. The vast number of hypothetical open framework structures that have yet to be synthetically realized point to a design space for materials discovery that is virtually limitless, provided the technical barriers for characterization can be overcome and knowledge gaps are sufficiently addressed. Indeed, the voids in our understanding of nucleation of open framework materials still loom large.

https://doi.org/10.1557/mrs.2016.89 Published online by Cambridge University Press

Acknowledgments

We are grateful to W.R. Dichtel and M. Dincă for providing valuable information on COFs and MOFs. J.D.R. acknowledges support from the National Science Foundation (Award 1151098), the Welch Foundation (Award E-1794), and the US Department of Energy, Office of Basic Energy Sciences (Award DE-SC0014468). M.T. acknowledges support from the Center for Gas Separations Relevant to Clean Energy Technologies, an Energy Frontier Research Center funded by the US Department of Energy, Office of Science, Office of Basic Energy Sciences (Award DE-SC0001015).

References

1. http://www.iza-structure.org/databases.
2. M. Dincă, A. Dailly, Y. Liu, C.M. Brown, D.A. Neumann, J.R. Long, *J. Am. Chem. Soc.* **128**, 16876 (2006).
3. H. Furukawa, K.E. Cordova, M. O'Keeffe, O.M. Yaghi, *Science*, **341**, 974 (2013).
4. B.J. Smith, N. Hwang, A.D. Chavez, J.L. Novotney, W.R. Dichtel, *Chem. Commun.* **51**, 7532 (2015).
5. Y.Z. Liu, C.H. Hu, A. Comotti, M.D. Ward, *Science* **333**, 436 (2011).
6. M.E. Davis, *Nature* **417**, 813 (2002).
7. C. Martinez, A. Corma, *Coord. Chem. Rev.* **255**, 1558 (2011).
8. M.A. Snyder, M. Tsapatsis, *Angew. Chem. Int. Ed.* **46**, 7560 (2007).
9. O.M. Yaghi, M. O'Keeffe, N.W. Ockwig, H.K. Chae, M. Eddaoudi, J. Kim, *Nature* **423**, 705 (2003).
10. A. Corma, H. Garcia, F. Xamena, *Chem. Rev.* **110**, 4606 (2010).
11. A.P. Cote, A.I. Benin, N.W. Ockwig, M. O'Keeffe, A.J. Matzger, O.M. Yaghi, *Science* **310**, 1166 (2005).
12. R.E. Morris, J. Cejka, *Nat. Chem.* **7**, 381 (2015).
13. M.W. Deem, R. Pophale, P.A. Cheeseman, D.J. Earl, *J. Phys. Chem. C* **113**, 21353 (2009).
14. Y.J. Colon, R.Q. Snurr, *Chem. Soc. Rev.* **43**, 5735 (2014).
15. A. Corma, F. Rey, J. Rius, M.J. Sabater, S. Valencia, *Nature* **431**, 287 (2004).
16. J.D. Rimer, M. Kumar, R. Li, A.I. Lupulescu, M.D. Oleksiak, *Catal. Sci. Technol.* **4**, 3762 (2014).
17. C.E. Wilmer, M. Leaf, C.Y. Lee, O.K. Farha, B.G. Hauser, J.T. Hupp, R.Q. Snurr, *Nat. Chem.* **4**, 83 (2012).
18. B.J. Smith, W.R. Dichtel, *J. Am. Chem. Soc.* **136**, 8783 (2014).
19. J.J. De Yoreo, P. Gilbert, N. Sommerdijk, R.L. Penn, S. Whitelam, D. Joester, H.Z. Zhang, J.D. Rimer, A. Navrotsky, J.F. Banfield, A.F. Wallace, F.M. Michel, F.C. Meldrum, H. Colfen, P.M. Dove, *Science* **349**, 498 (2015).
20. D. Kashchiev, *J. Chem. Phys.* **118**, 1837 (2003).
21. C.S. Cundy, P.A. Cox, *Microporous Mesoporous Mater.* **82**, 1 (2005).
22. O. Galkin, P.G. Vekilov, *Proc. Natl. Acad. Sci. U.S.A.* **97**, 6277 (2000).
23. P.G. Vekilov, *Cryst. Growth Des.* **10**, 5007 (2010).
24. J.D. Rimer, D.G. Vlachos, R.F. Lobo, *J. Phys. Chem. B* **109**, 12762 (2005).
25. P. de Moor, T.P.M. Beelen, R.A. van Santen, *J. Phys. Chem. B* **103**, 1639 (1999).
26. N.D. Hould, R.F. Lobo, *Chem. Mater.* **20**, 5807 (2008).
27. M. Maldonado, M.D. Oleksiak, S. Chinta, J.D. Rimer, *J. Am. Chem. Soc.* **135**, 2641 (2013).
28. N. Ren, B. Subotic, J. Bronic, Y. Tang, M.D. Sikiric, T. Misic, V. Svetlicic, S. Bosnar, T.A. Jelic, *Chem. Mater.* **24**, 1726 (2012).
29. S. Mintova, N.H. Olson, T. Bein, *Angew. Chem. Int. Ed.* **38**, 3201 (1999).
30. S. Mintova, N.H. Olson, V. Valtchev, T. Bein, *Science* **283**, 958 (1999).
31. T.M. Davis, T.O. Drews, H. Ramanan, C. He, J.S. Dong, H. Schnablegger, M.A. Katsoulakis, E. Kokkoli, A.V. McCormick, R.L. Penn, M. Tsapatsis, *Nat. Mater.* **5**, 400 (2006).
32. J.M. Fedeyko, J.D. Rimer, R.F. Lobo, D.G. Vlachos, *J. Phys. Chem. B* **108**, 12271 (2004).
33. S. Kumar, T.M. Davis, H. Ramanan, R.L. Penn, M. Tsapatsis, *J. Phys. Chem. B* **111**, 3398 (2007).
34. J.D. Rimer, R.F. Lobo, D.G. Vlachos, *Langmuir* **21**, 8960 (2005).
35. S.-C. Chien, S.M. Auerbach, P.A. Monson, *Langmuir* **31**, 4940 (2015).
36. D.D. Kragten, J.M. Fedeyko, K.R. Sawant, J.D. Rimer, D.G. Vlachos, R.F. Lobo, M. Tsapatsis, *J. Phys. Chem. B* **107**, 10006 (2003).
37. J.D. Rimer, O. Trofymluk, A. Navrotsky, R.F. Lobo, D.G. Vlachos, *Chem. Mater.* **19**, 4189 (2007).
38. S. Kumar, Z.P. Wang, R.L. Penn, M. Tsapatsis, *J. Am. Chem. Soc.* **130**, 17284 (2008).
39. L. Karwacki, M.H.F. Kox, D.A.M. de Winter, M.R. Drury, J.D. Meeldijk, E. Stavitski, W. Schmidt, M. Mertens, P. Cubillas, N. John, A. Chan, N. Kahn, S.R. Bare, M. Anderson, J. Kornatowski, B.M. Weckhuysen, *Nat. Mater.* **8**, 959 (2009).
40. R.L. Penn, J.F. Banfield, *Science* **281**, 969 (1998).
41. D.S. Li, M.H. Nielsen, J.R.I. Lee, C. Frandsen, J.F. Banfield, J.J. De Yoreo, *Science* **336**, 1014 (2012).
42. A. Malani, S.M. Auerbach, P.A. Monson, *J. Phys. Chem. C* **115**, 15988 (2011).
43. T. Verstraelen, B.M. Szyja, D. Lesthaeghe, R. Declerck, V. Van Speybroeck, M. Waroquier, A.P.J. Jansen, A. Aerts, L.R.A. Follens, J.A. Martens, C.E.A. Kirschhock, R.A. van Santen, *Top. Catal.* **52**, 1261 (2009).
44. C.-S. Yang, J.M. Mora-Fonz, C.R.A. Catlow, *J. Phys. Chem. C* **116**, 22121 (2012).
45. X.-Q. Zhang, T.T. Trinh, R.A. van Santen, A.P.J. Jansen, *J. Am. Chem. Soc.* **133**, 6613 (2011).
46. C.S. Yang, J.M. Mora-Fonz, C.R.A. Catlow, *J. Phys. Chem. C* **117**, 24796 (2013).
47. M.B. Park, Y. Lee, A.M. Zheng, F.S. Xiao, C.P. Nicholas, G.J. Lewis, S.B. Hong, *J. Am. Chem. Soc.* **135**, 2248 (2013).
48. D. Lesthaeghe, P. Vansteenkiste, T. Verstraelen, A. Ghysels, C.E.A. Kirschhock, J.A. Martens, V. Van Speybroeck, M. Waroquier, *J. Phys. Chem. C* **112**, 9186 (2008).
49. B.B. Schaack, W. Schrader, T. Schuth, *Angew. Chem. Int. Ed.* **47**, 9092 (2008).
50. L.R.A. Follens, A. Aerts, M. Haouas, T.P. Caremans, B. Loppinet, B. Goderis, J. Vermant, F. Taulelle, J.A. Martens, C.E.A. Kirschhock, *Phys. Chem. Chem. Phys.* **10**, 5574 (2008).
51. L. Jin, S.M. Auerbach, P.A. Monson, *J. Phys. Chem. Lett.* **3**, 761 (2012).
52. S. Caratzoulas, D.G. Vlachos, M. Tsapatsis, *J. Am. Chem. Soc.* **128**, 596 (2006).
53. A. Navrotsky, O. Trofymluk, A.A. Levchenko, *Chem. Rev.* **109**, 3885 (2009).
54. D. Wu, A. Navrotsky, *J. Solid State Chem.* **223**, 53 (2015).
55. K.S. Park, Z. Ni, A.P. Cote, J.Y. Choi, R.D. Huang, F.J. Uribe-Romo, H.K. Chae, M. O'Keeffe, O.M. Yaghi, *Proc. Natl. Acad. Sci. U.S.A.* **103**, 10186 (2006).
56. A. Navrotsky, *Proc. Natl. Acad. Sci. U.S.A.* **101**, 12096 (2004), doi:10.1073/pnas.0404778101.
57. M.Y. Li, M. Dincă, *Chem. Mater.* **27**, 3203 (2015).
58. M. Oleksiak, J.D. Rimer, *Rev. Chem. Eng.* **30**, 1 (2014).
59. B. Xie, H.Y. Zhang, C.G. Yang, S.Y. Liu, L.M. Ren, L. Zhang, X.J. Meng, B. Yilmaz, U. Muller, F.S. Xiao, *Chem. Commun.* **47**, 3945 (2011).
60. K. Itabashi, Y. Kamimura, K. Iyoki, A. Shimojima, T. Okubo, *J. Am. Chem. Soc.* **134**, 11542 (2012).
61. P. Eliášová, M. Opanasenko, P.S. Wheatley, M. Shamzhy, M. Mazur, P. Nachtigall, J.W. Roth, R.E. Morris, J. Čejka, *Chem. Soc. Rev.* **44**, 7177 (2015).
62. S.L. Burkett, M.E. Davis, *J. Phys. Chem.* **98**, 4647 (1994).
63. B.J. Schoeman, J. Sterte, J.E. Otterstedt, *Zeolites* **14**, 568 (1994). □



https://doi.org/10.1557/mrs.2016.89 Published online by Cambridge University Press